Received: 6 April 2023 | Accepted: 23 August 2023

DOI: 10.1097/HC9.0000000000000299

ORIGINAL ARTICLE

OPEN

HMGB2 is a potential diagnostic marker and therapeutic target for liver fibrosis and cirrhosis

Yi Huang[1] | Suthat Liangpunsakul[2,3] | Swetha Rudraiah[1] | Jing Ma[2] | Santosh K. Keshipeddy[4] | Dennis Wright[4] | Antonio Costa[4] | Diane Burgess[4] | Yuxia Zhang[5] | Nazmul Huda[2] | Li Wang[6] | Zhihong Yang[2]

[1]Department of Physiology and Neurobiology, University of Connecticut, Storrs, Connecticut, USA

[2]Department of Medicine, Division of Gastroenterology and Hepatology, Indiana University, Indianapolis, Indiana, USA

[3]Medicine Service, Roudebush Veterans Administration Medical Center, Indianapolis, Indiana, USA

[4]Department of Pharmaceutical Sciences, School of Pharmacy, University of Connecticut, Storrs, Connecticut, USA

[5]Department of Pharmacology, Toxicology, and Therapeutics, University of Kansas Medical Center, Kansas City, Kansas, USA

[6]Department of Pharmacology and Toxicology, College of Pharmacy, University of Arizona, Tucson, Arizona, USA

Correspondence
Zhihong Yang, Division of Gastroenterology and Hepatology, Department of Medicine, Indiana University School of Medicine, 702 Rotary circle, Indianapolis, IN 46202.
Email: yangjoe@iu.edu

Abstract

Background: High mobility group proteins 1 and 2 (HMGB1 and HMGB2) are 80% conserved in amino acid sequence. The function of HMGB1 in inflammation and fibrosis has been extensively characterized. However, an unaddressed central question is the role of HMGB2 on liver fibrosis. In this study, we provided convincing evidence that the HMGB2 expression was significantly upregulated in human liver fibrosis and cirrhosis, as well as in several mouse liver fibrosis models.

Methods: The carbon tetrachloride (CCl_4) induced liver fibrosis mouse model was used. AAV8-Hmgb2 was utilized to overexpress Hmgb2 in the liver, while *Hmgb2*$^{-/-}$ mice were used for loss of function experiments. The HMGB2 inhibitor inflachromene and liposome-shHMGB2 (lipo-shHMGB2) were employed for therapeutic intervention.

Results: The serum HMGB2 levels were also markedly elevated in patients with liver fibrosis and cirrhosis. Deletion of Hmgb2 in *Hmgb2*$^{-/-}$ mice or inhibition of HMGB2 in mice using a small molecule ICM slowed the progression of CCl_4-induced liver fibrosis despite constant HMGB1 expression. In contrast, AAV8-mediated overexpression of Hmgb2 enchanced CCl_4-incuded liver fibrosis. Primary hepatic stellate cells (HSCs) isolated from *Hmgb2*$^{-/-}$ mice showed significantly impaired transdifferentiation and diminished activation of α-SMA, despite a modest induction of HMGB1 protein. RNA-seq analysis revealed the induction of top 45 CCl_4-activated genes in multiple signaling

Abbreviations: α-SMA, alpha smooth muscle actin; AAV8-Con, AAV8-Hmgb2 or control AAV8; AST, aspartate aminotransferase; AKT, akt kinase (also called protein kinase B, PKB); BSA, bovine serum albumin; CCl_4, carbon tetrachloride; Ccnb2, cyclin B; *Col1a1*, collagen type I alpha; Cx3cr1, C-X3-C motif chemokine receptor 1; ECM, extracellular matrix; ERK, extracellular signal-regulated kinase; Fbn, fibrillin; *Fbn2*, fibrillin2; Fmod, fibromodulin; GO, gene ontology; HBSS, Hank balanced salt solution; HCFD, high cholesterol and saturated fat diet; HMGB1, high mobility group protein 1; HMGB2, high mobility group protein 2; ICM, inflachromene; LPS, lipopolysaccharide; LX-2 cell line, Lieming Xu-2 cell line; MMP, metalloproteinases; PANTHER, protein annotation through evolutionary relationship; PDGF, platelet-derived growth factor; qPCR, quantitative PCR; *Racgap1*, Rac GTPase-activating protein 1; RANTES, regulated upon activation, normal T cell expressed and secreted; STRING, search tool for the retrieval of interacting genes/protein; *Top2a*, topoisomerase 2-alpha; WB, western blot; WT, wild type.

Supplemental Digital Content is available for this article. Direct URL citations are provided in the HTML and PDF versions of this article on the journal's website, www.hepcommjournal.com.

pathways including integrin signaling and inflammation. The activation of these genes by CCl_4 were abolished in *Hmgb2*$^{-/-}$ mice or in ICM-treated mice. These included C-X3-C motif chemokine receptor 1 (Cx3cr1) associated with inflammation, cyclin B (Ccnb) associated with cell cycle, DNA topoisomerase 2-alpha (Top2a) associated with intracellular component, and fibrillin (Fbn) and fibromodulin (Fmod) associated with extracellular matrix.

Conclusion: We conclude that HMGB2 is indispensable for stellate cell activation. Therefore, HMGB2 may serve as a potential therapeutic target to prevent HSC activation during chronic liver injury. The blood HMGB2 level may also serve as a potential diagnostic marker to detect early stage of liver fibrosis and cirrhosis in humans.

INTRODUCTION

Liver fibrosis is characterized by the excessive accumulation of extracellular matrix (ECM) in response to liver injury, which is mainly produced by HSCs. Liver fibrosis can progress to cirrhosis, portal hypertension, and HCC, leading to increased morbidity and mortality.[1] Upon liver injury, quiescent HSCs become activated to express alpha smooth muscle actin (α-SMA), undergoing transdifferentiation into myofibroblast-like cells that exhibit the ability to proliferate and produce profibrogenic ECM components.[2] Studies have shown that platelet-derived growth factor (PDGF) and TGF-β are critical mediators of HSC activation.[3] Additionally, other molecules including p38 MAPK, extracellular signal-regulated kinase (ERK), and inflammatory cytokines such as TNF-α, IL-1β, and IL-6 are implicated in HSC activation.[4–6] However, the molecular basis underlying the interplay remains poorly understood.

High mobility group box 2 (HMGB2) is a highly conserved nuclear protein in mammals.[7] It is a member of HMGB proteins that contain 2 DNA-binding domains, HMG A-box and HMG B-box, and a long acidic carboxyl-terminal tail. In the nucleus, HMGB proteins preferentially bind to a minor groove of DNA in a nonspecific manner. The binding induces the conformational changes of DNA, facilitating the assembly of multiprotein complexes including transcription factors. As DNA architectural factors, HMGB proteins function in DNA replication, recombination, transcription, repair, and stem cell differentiation.[8,9] HMGB2 interacts with several proteins, including SET nuclear proto-oncogene (SET), tumor protein P53, steroid hormone receptors, and steroid receptor coactivator-1, to be involved in chromatin binding and DNA repair.[10,11]

Although the HMGB2 protein was initially discovered to be localized in the nucleus, a recent study has demonstrated the translocation of HMGB2 from the nucleus to the cytoplasm, where HMGB2 underwent phosphorylation or acetylation in response to lipopolysaccharide (LPS) in microglia cells.[12] Moreover, HMGB2 is present in the extracellular milieu.[12] HMGB2 is released by human leukemia monocyte THP-1 cells after LPS stimulation, and extracellular HMGB2 is detected in an *in vivo* experimental autoimmune encephalomyelitis model and LPS-induced acute lung injury, implicating its potential role in the inflammatory response.[13,14] HMGB2 expression is ubiquitous during embryogenesis, whereas it is primarily expressed in lymphoid organs and testis in adult mice.[15] Mice lacking *Hmgb2* (*Hmgb2*$^{-/-}$) are viable; however, they display reduced chondrocyte cellularity and myogenesis.[16,17] Male mice homozygous for *Hmgb2* deletion display reduced fertility.[15]

A recent study reports that HMGB2 is overexpressed in HCC.[18] However, little is known about its regulatory role in liver function and nonmalignant liver diseases. In this study, we have uncovered a critical indispensable role of HMGB2 in stellate cell activation associated with toxin-induced liver fibrosis.

METHODS

Human specimens and animals

Deidentified human liver specimens were obtained through the Liver Tissue Cell Distribution System (Minneapolis, MN) funded by NIH Contract # HSN276201200017C, as described.[19–21] The human plasma or serum samples were collected from Yale Liver Center and Indiana University.[22,23] The study was approved by the Institutional Review Board at the Indiana University Purdue University Indianapolis. Written informed consent was obtained from each participant. All animal care and experimental procedures were approved by the Institutional Animal Care and Use Committee at the University of Connecticut.

Hmgb2$^{-/-}$ mice and their siblings were used for feeding experiments. For carbon tetrachloride (CCl_4) treatment, CCl_4 (Sigma) was dissolved in corn oil and administered to mice at a dose of 850 μL/kg body weight by i.p. injection twice a week from 6 to 12 weeks. Age-matched control mice were treated with a corn oil vehicle. For HMGB2 inhibitor inflachromene (ICM)[12] treatment, mice were initially treated with CCl_4 for 2 weeks followed by ICM dissolved in polyethylene glycol (Sigma) at the dose of 10 mg/kg body weight daily for 4 weeks concurrently with CCl_4. The alcohol plus CCl_4 treatment model was modified and adapted from a previous publication.[24] In brief, the wild-type female (8 wk) mice were fed with a 5% ethanol diet for 1 month, and injected 400 μL/kg CCl_4 or PBS twice per week for the last 2 weeks. The high cholesterol and saturated fat diet (HCFD) and alcohol feeding plus 1 binge models were described.[25] To generate Hmgb2 overexpressing mice, AAV8-Hmgb2 or control AAV8 (AAV8-Con)[26] was given to mice by tail vein injection at a dose of 5×10^{10} genome copy number/mL (Penn Vector Core). To knockdown HMGB2 in mouse stellate cells, liposome-mediated delivery of shHmgb2 plasmid[27] was used. The sequences of the shHmgb2 are provided in Supplemental Table S1, http://links.lww.com/HC9/A606. Also see Supplemental Figure S2, http://links.lww.com/HC9/A607, and S3, http://links.lww.com/HC9/A607, for detailed schematic diagrams.

Livers were removed and snap-frozen in liquid nitrogen for RNA and protein analysis. For the collection of mouse fetal livers, pregnant female mice were sacrificed at E12.5, E15, and E18.5 and livers were removed from the embryos. Additionally, postnatal mouse livers were harvested at postnatal days P1 and P60. Serum alanine transaminase and aspartate aminotransferase (AST) were measured by Infinity alanine transaminase and AST liquid stable reagent according to the manufacturer's instructions (Thermo Scientific), as described.[28,29]

Mouse primary HSC isolation and in vitro culture activation

Primary mouse HSCs were isolated from 8- to 12-weeks-old wild-type (WT) or *Hmgb2*$^{-/-}$ mice, as described with some modifications.[28,30] Briefly, mice were anesthetized with a ketamine/xylazine mixture. The liver was perfused with Hank balanced salt solution (HBSS) supplemented with 0.5 mM EGTA through the cannulated portal vein, followed by perfusion with HBSS supplemented with 0.5 mg/mL pronase (Sigma) and HBSS with 0.14 mg/mL collagenase (Sigma). The liver was dissected out from the mice and the dissociated cells were dispersed gently in HBSS. Primary HSCs were isolated by 3-layer discontinuous density gradient centrifugation with 25% and 50% percoll (Sigma) and plated on noncoated culture dishes in DMEM supplemented with 10% fetal bovine serum, 100 IU/mL penicillin, and 100 μg/mL streptomycin. For culture-activated HSC studies, the medium of primary HSCs was replaced every day up to 7 days. For the profibrotic mediators' treatment, primary HSC cells culture-activated at day 5 were serum-starved for 24 hour and then treated with PDGF (50 ng/mL), RANTES (50 ng/mL), LPS (100 ng/mL), and TGF-β (10 ng/mL) for 5 minutes.

Immunofluorescence

Primary mouse HSCs were plated on coverslips and culture-activated, fixed with 4% paraformaldehyde for 15 minutes, and blocked in PBS containing 5% normal serum and 0.3% Triton X-100 for 60 minutes. Cells were incubated with a primary antibody for HMGB2 or α-SMA in PBS containing 1% BSA and 0.3% Triton X-100 overnight at 4°C. After 5 washes with PBS, cells were incubated with a secondary antibody for goat anti-rabbit Alexa Fluor 594 conjugate (Thermo Fisher) or goat anti-mouse Alexa Fluor 488 conjugate (Thermo Fisher). Co-staining of HMGB2 and Desmin or α-SMA used rabbit anti-HMGB2 (ab 67282, Abcam), goat anti-Desmin (AF3844, R&D systems), and mouse anti-α-SMA (ab7817, Abcam). The secondary antibodies of goat anti-rabbit Alexa Fluor 594, goat anti-rabbit Alexa Fluor 488, donkey anti-goat Alexa Fluor 488, and goat anti-mouse Alexa Fluor 594 (Thermo Fisher) were used. Slides were washed with PBS and mounted with mounting media containing DAPI.

ELISA

The levels of HMGB2 in plasma samples from mice treated with CCl_4 and serum samples from patients who were associated with liver diseases were determined using ELISA kits (LifeSpan BioSciences) according to the manufacturer's instructions.

RNA sequencing and bioinformatics

The sequencings were performed using the Illumina RNA sequencing protocol. RNA-seq reads were aligned to the mouse reference genome (GRCm38/mm10). The log-transformed reads of the differentially expressed genes were normalized to the average of WT-oil within each dataset. Genes with a log-transformed false discovery rate of >13 (equal to untransformed false discovery rate of <0.05 or <5 false positives per 100 observations) and Log2FC (fold change) >1 were considered as significantly differentially expressed. The heatmap, volcano plot, and Venn diagram were generated using the R package (version 3.3.1). The pathways

were analyzed using the PANTHER (protein annotation through evolutionary relationship) classification system (Version 11). The original sequencing data were submitted to NCBI with an access number of GSE 98577.

Protein-protein interaction network analysis

To understand the interaction network of HMGB2-regulated genes, we submitted the top 45 most differentially expressed genes to the online STRING v 10.5 database (http://string-db.org/) to retrieve interactions pertaining to those genes. We filtered the network with a high confidence score of >0.9, which signifies $>80\%$ probability that these interactions may be replicated in the Kyoto Encyclopedia of Genes and Genomes database.[20] Molecular action was chosen to represent the interactions. Additionally, the interactors were grouped into 5 clusters based on shared similarity/relatedness, using the k-means algorithm provided by the STRING database.

Other standard methods

The LX-2 human stellate cell line was cultured as described.[31] In brief, the LX-2 cells were maintained in DMEM supplemented with 2% fetal bovine serum, 100 IU/mL penicillin, and 100 μg/mL streptomycin. Cells were maintained at a 37°C humidified atmosphere with 5% CO_2. Western blot (WB), quantitative PCR (qPCR), *in vitro* virus transduction and plasmid transfection, liver histology, hepatic lipid extraction and blood chemistry, immunocytochemistry, and confocal images were described.[32–39] The primer sequences for qPCR are provided in Supplemental Table S2, http://links.lww.com/HC9/A606. For WB analyses, equal amounts of protein from livers in each group (n = 5 or 10 mice/group) were pooled, and single or duplicate loading was used unless otherwise indicated. The following antibodies were obtained from Cell Signaling Technology (Danvers, MA): HMGB2 (#14163 for WB), HMGB1 (#6893), AKT (#4691), p-AKT (#4051), ERK1/2 (#8690), pERK1/2 (#4370), Smad4 (#9515), p-Smad2/3 (#8828), Lamin A/C (#4777), and α-SMA (#14968). Antibodies against metalloproteinases (MMP)2 (#AF980), MMP9 (#AF1488), and TIMP1 (#AF909) were obtained from R&D Systems (Minneapolis, MN). An anti-HA antibody and an anti-beta actin antibody were purchased from Sigma and Santa Cruz Biotechnology, respectively. For quantification of Masson Trichrome staining, 8 images were randomly chosen and submitted to Image J (version 2.0.0-rc-43/1.50 g) analysis.[40] Positive areas were selected, and the relative intensity was calculated and compared with the control group.

Statistical analysis

Data were expressed as the mean ± SEM. All data are representative of at least 3 independent experiments. Statistical analysis was carried out using Student *t* test between 2 groups and 1-way ANOVA among multiple groups. $p<0.05$ was considered statistically significant.

RESULTS

HMGB2 expression is markedly induced in human and murine hepatic fibrosis

To establish the clinical relevance of HMGB2, we analyzed HMGB2 mRNA in human liver specimens from patients with various chronic liver diseases. HMGB1 mRNA was significantly induced in liver samples from patients with liver fibrosis, NASH, alcohol-associated cirrhosis, and HCV cirrhosis, but not in patients with steatosis (Figure 1A). The patient's biometric and diagnostic summaries were provided in Supplemental Table S3, http://links.lww.com/HC9/A664. From the samples in Figure 1A, 4 samples from normal, NASH cirrhosis, and alcohol-associated cirrhosis were randomly selected to determine HMGB2 protein levels. The expression of HMGB2 protein was also markedly elevated in the liver specimens from patients with NASH and alcohol-induced cirrhosis, corresponding with the induction of its mRNA (Figure 1B left vs. right). In addition, immunofluorescence staining revealed markedly increased HMGB2 protein expression in human fibrotic and cirrhotic livers (Figure 1C).

In mice, hepatic *Hmgb2* mRNA expression was high during the embryonic stage, but its levels drastically decreased in adulthood (Supplemental Figure S1A, http://links.lww.com/HC9/A607), as revealed by RNA-seq (left) and validated by qPCR (right). Interestingly, hepatic HMGB2 protein was markedly elevated during liver injury induced by CCl_4 plus alcohol feeding (Figure 1D–F). By co-staining HMGB2 with DESMIN or α-SMA, a well-known marker for liver fibrosis, we observed that HMGB2 was enriched in the fibrotic area and presented in fibrotic cells in CCl_4+alcohol mouse liver (Figure 1F) and human alcohol-associated cirrhosis liver (Supplemental Figure S1B, http://links.lww.com/HC9/A607). Similarly, HMGB2 protein was significantly upregulated in HCFD, HCFD with alcohol, and HCFD with alcohol plus binge (Supplemental Figure S1C, http://links.lww.com/HC9/A607) mice livers. The degree of its upregulation positively correlated with the severity of liver inflammation and fibrosis.

The cytoplasmic localization of HMGB2 indicated its extracellular secretion, thus we determined serum HMGB2 levels in patients with liver fibrosis and cirrhosis. Overall, serum HMGB2 levels were markedly increased in patients with HCV, NAFLD fibrosis, and other types of

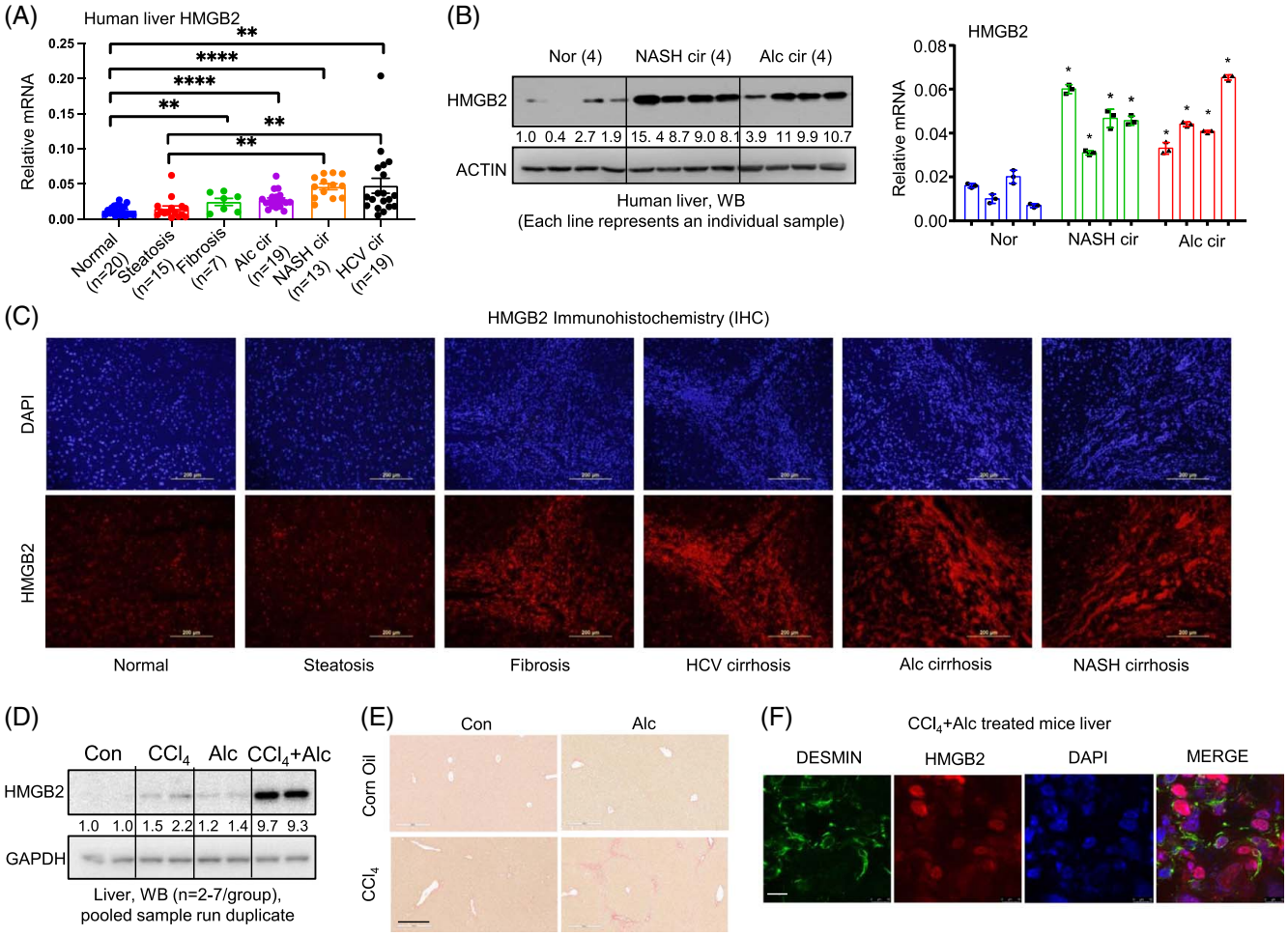

FIGURE 1 The expression of HMGB2 is highly induced in human and mouse fibrotic livers. (A) Quantitative PCR of *HMGB2* mRNA in human liver specimens from patients with steatosis (n = 15), fibrosis (n = 7), alcohol-associated cirrhosis (n = 19), NASH cirrhosis (n = 13), and HCV cirrhosis (n = 19), which was normalized by *HPRT1*. Data are shown as mean ± SEM. $^{**}p < 0.01$; $^{****}p < 0.0001$ versus indicated group. (B) Western blot of HMGB2 protein (left) and quantitative PCR of *HMGB2* mRNA (right) in human liver specimens (n = 4) from samples in A. $^{*}p < 0.05$ versus normal. (C) IHC analysis of HMGB2 protein expression in human cirrhotic livers. Scale bar = 200 μm. (D–F) Wild-type female mice were fed with 5% ethanol or a control diet for 1 month. 0.4 mL/kg CCl_4 was injected twice per week for the last 2 weeks. The mice were harvested for the WB (D) and Sirius red staining (E). Scale bar: 300 μm. (F) Immunofluorescence co-staining of HMGB2 (Red) and DESMIN (Green) in alcohol plus CCl_4–treated mice in (D–F). The nuclear was stained with DAPI (Blue). Scale bar = 10 μm. Abbreviations: Alc, alcohol; CCl_4, carbon tetrachloride; HMGB2, high mobility group protein 2; IHC, immunohistochemistry; WB, western blot. Note: DESMIN (Green) was used as fibrosis marker. GAPDH was used as loading control.

liver fibrosis (Figure 2A–C). The increases were observed from the early stages (I and II) and were persistent to the late stages. Interestingly, the HMGB2 levels were more strikingly increased in Child A and B compared to Child C in alcohol-associated liver cirrhosis (Figure 2D), suggesting the severity of cirrhosis likely affected HMGB2 secretion or protein degradation. The results demonstrate an important regulatory role of HMGB2 in liver fibrosis and cirrhosis in both humans and mice.

Overexpression of HMGB2 enhances, whereas Hmgb2 deficiency prevents liver fibrosis

Adeno-associated virus AAV8-mediated gene delivery[41] showed a long-lasting effect with no inflammation as compared to adenovirus. We generated AAV8-Hmgb2 to deliver the Hmgb2 into WT mice with the same background as *Hmgb2*$^{-/-}$ mice. WT control mice and AAV8-Hmgb2–injected WT mice, as well as *Hmgb2*$^{-/-}$ mice were used for the CCl_4-induced liver fibrosis model. One week after administration of AAV8-Hmgb2 or control virus via the tail vein in the WT mice, WT control mice, AAV8-Hmgb2 WT mice, and *Hmgb2*$^{-/-}$ mice were injected with CCl_4 or corn oil for 6 weeks. Animals were sacrificed and tissues were harvested 72 hour after the last injection. The confirmation of HMGB2 overexpression and deletion is presented in Supplemental Figure S1D, http://links.lww.com/HC9/A607.

Masson Trichrome staining and quantification of fibrosis areas revealed that ectopic expression of Hmgb2 enhanced fibrogenesis induced by CCl_4 (CCl_4/AAV8-Hmgb2 vs. CCl_4/AAV8-Con). In contrast, *Hmgb2*$^{-/-}$ mice

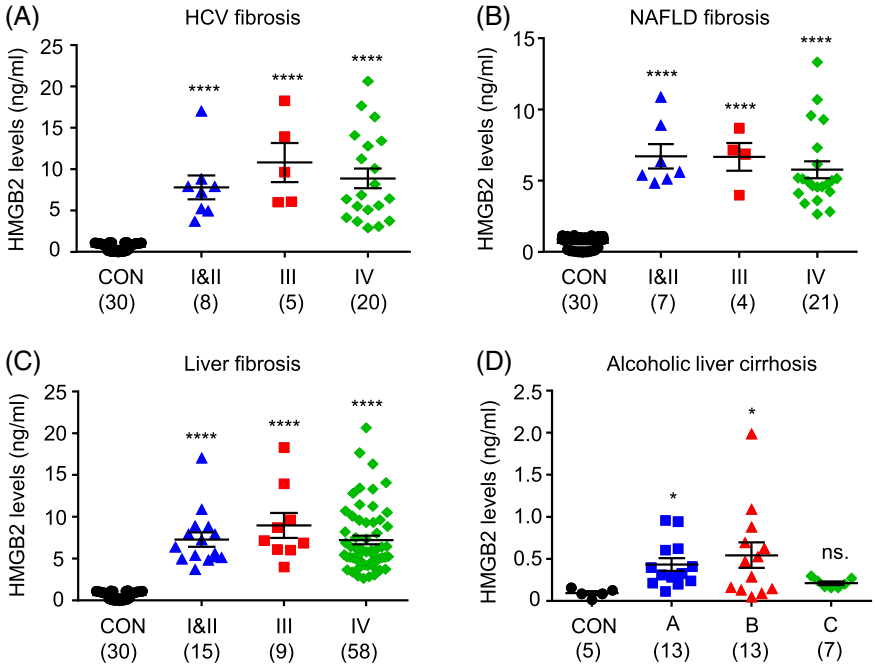

FIGURE 2 HMGB2 protein levels in the blood are elevated in human liver diseases. (A–D) ELISA of serum HMGB2 levels in patients with different stages of HCV fibrosis (A), NAFLD fibrosis (B), liver fibrosis (C), and alcohol-associated liver cirrhosis (Child A, B, C) (D). Samples were collected from Yale Liver Center (A-C) and Indiana University (D). $^{*}p < 0.05$; $^{****}p < 0.0001$ versus CON (healthy control). Abbreviation: HMGB2, high mobility group protein 2.

treated with CCl_4 did not develop fibrosis (CCl_4/*Hmgb2*$^{-/-}$ vs. CCl_4/AAV8-Con) (Figure 3A). Consistently, CCl_4 increased the protein expression of α-SMA, a marker for the transdifferentiation of HSC to myofibroblast-like cells, in WT mice, which was further enhanced in AAV8-Hmgb2 mice but diminished in *Hmgb2*$^{-/-}$ mice (Figure 3B). CCl_4 treatment elevated plasma alanine transaminase and AST levels, which were further increased in AAV8-Hmgb2 mice and diminished in *Hmgb2*$^{-/-}$ mice (Figure 3C). Overall, overexpression of HMGB2

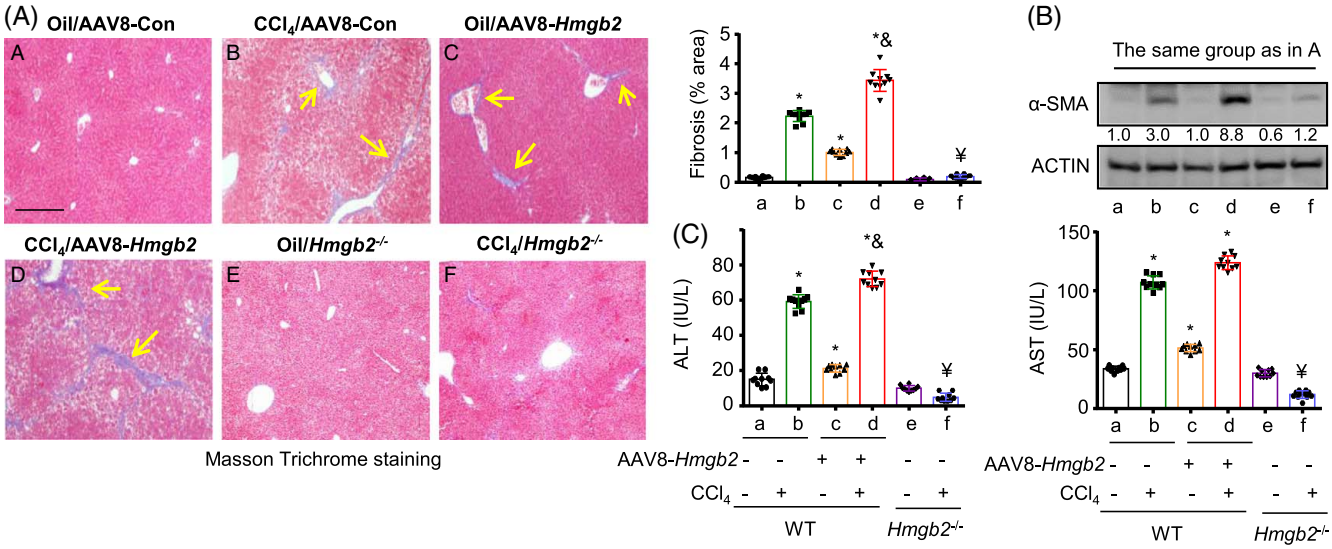

FIGURE 3 Overexpression of Hmgb2 facilitates, whereas Hmgb2 deficiency prevents CCl_4-induced liver fibrosis. (A) Representative images of Masson Trichrome staining of liver sections. WT mice that had the same background as *Hmgb2*$^{-/-}$ mice were transduced with AAV8-GFP or AAV8-Hmgb2 via tail vein injection for 1 week. These mice and *Hmgb2*$^{-/-}$ mice were i.p. injected with corn oil or CCl_4 for 6 weeks (n = 6 mice/group). Top right: Quantification of fibrosis in A. Scale bar = 300 μm. (B) Western blot of α-SMA protein from livers of WT, AAV8-Hmgb2, and *Hmgb2*$^{-/-}$ mice with or without CCl_4 in A. Each band represents a pooled sample (equal amounts of protein) from 6 individual mice. Quantification of the intensity of each band was performed using ImageJ software and is provided under each line. (C) Plasma levels of ALT and AST. $^{*}p < 0.05$ versus a; $^{\&}p < 0.05$ versus b; $^{¥}p < 0.05$ versus c. Abbreviations: α-SMA, alpha smooth muscle actin; AAV8-Con, AAV8-Hmgb2 or control AAV8; ALT, alanine transaminase; AST, aspartate aminotransferase; CCl_4, carbon tetrachloride; HMGB2, high mobility group protein 2; WT, wild type.

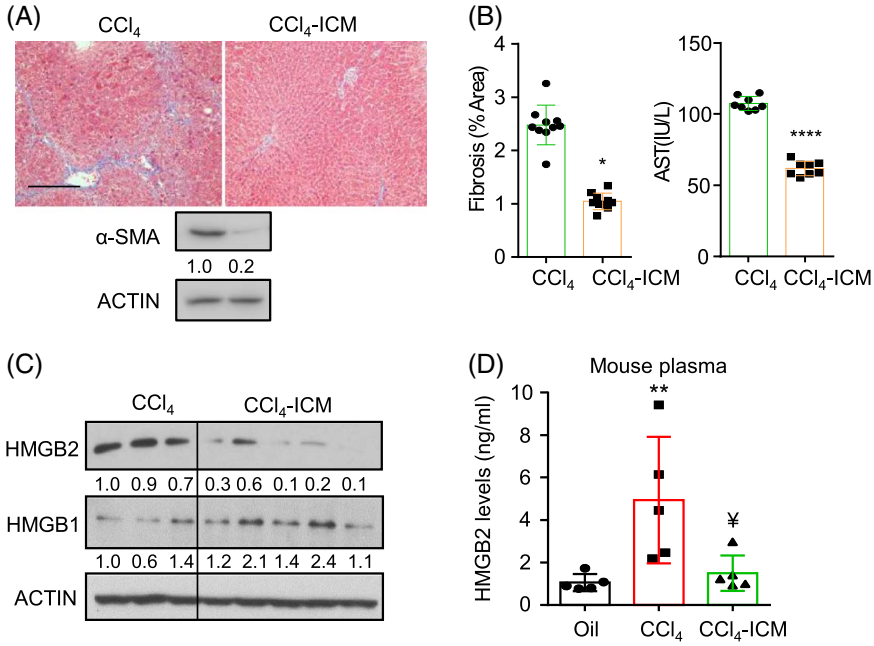

FIGURE 4 Inhibition of Hmgb2 protects mice from CCl_4-induced liver fibrosis. (A) Top: Representative images of Masson Trichrome staining of liver sections in CCl_4 and CCl_4+ICM mice. Bottom: Western blots of α-SMA protein. Each band represents pooled samples from 3 (CCl_4) and 5 (CCl_4+ICM) individual mice, respectively. Scale bar = 300 μm. (B) Quantification of fibrosis areas and plasma AST levels (n = 5–10/group). Data are shown as mean ± SEM. *$p < 0.05$; ****$p < 0.0001$ versus CCl_4. (C) Western blot of HMGB2 and HMGB1 proteins in CCl_4 and CCl_4+ICM mice (CCl_4 group: n = 3; CCl_4+ICM group: n = 5). For all western blot: quantification of the intensity of each band was performed using ImageJ software and is provided under each line. (D) ELISA of plasma HMGB2 levels in mice treated with corn oil, CCl_4, or CCl_4 plus ICM for 6 weeks. **$p < 0.01$ CCl_4 versus oil; ¥$p < 0.05$ CCl_4/ICM versus CCl_4 (n = 5/group). Abbreviations: α-SMA, alpha smooth muscle actin; AST, aspartate aminotransferase; CCl_4, carbon tetrachloride; HMGB2, high mobility group protein 2; ICM, inflachromene.

enhances, whereas *Hmgb2* deficiency prevents CCl_4-induced liver injury and fibrosis.

A small molecule inhibitor of HMGB2 protects mice from developing liver fibrosis

We further examined the effect of a small molecule inhibitor of HMGB2, namely ICM, on the regulation of liver fibrosis. WT mice were treated with CCl_4 for 2 weeks, followed by the treatment of a combination of CCl_4 and ICM or vehicle polyethylene glycol for 4 weeks. The degree of hepatic fibrosis as determined by Masson Trichrome staining (Figure 4A top), α-SMA protein (Figure 4A bottom), and the degree of liver injury as determined by plasma AST levels (Figure 4B) were significantly improved in the ICM-treated group. ICM treatment significantly reduced HMGB2 protein levels with a modest opposite effect on HMGB1 protein expression (Figure 4C). ICM was reported to inhibit both HMGB2 and HMGB1 expressions in microglia.[12] However, our results showed that ICM only reduced HMGB2 but not HMGB1 protein in mouse livers, suggesting that it may work in a cell-type and tissue-type–dependent fashion. Since the plasma HMGB2 levels were elevated in fibrotic and cirrhotic livers in patients (Figure 2), we also determined HMGB2 levels in mouse plasma and observed its elevation by CCl_4, which were diminished by ICM treatment (Figure 4D). Overall, the results indicate that diminishing HMGB2 expression and function by ICM protects mice from developing liver fibrosis.

Next, we used liposome-mediated delivery of shHmgb2 in mouse liver to examine the effect of specific knockdown of HMGB2 in HSCs. The schematic of lipoplex is shown in Supplemental Figure S2A, http://links.lww.com/HC9/A607. Vitamin A extended from the surface to allow targeting hepatic stellate cells.[42] WT mice were treated with CCl_4 for 8 weeks followed by tail vein injection of liposome-shGfp or liposome-shHmgb2 for 4 weeks (Supplemental Figure S2B, http://links.lww.com/HC9/A607). Liver fibrosis examined by Masson Trichrome staining (Supplemental Figure S3A, http://links.lww.com/HC9/A607), serum AST levels (Supplemental Figure S3B, http://links.lww.com/HC9/A607), and α-SMA protein (Supplemental Figure S3C, http://links.lww.com/HC9/A607) were markedly decreased in liposome-shHmgb2 versus control mice. The knockdown efficiency of liposome-shHmgb2 to diminish Hmgb2, but not Hmgb1 mRNA expression, is presented in Supplemental Figure S4B, http://links.lww.com/HC9/A607.

Because liver fibrosis is often accompanied by inflammation, we examined the expression of genes in inflammatory pathways to clarify the hepatic responses to HMGB2 during CCl_4-induced injury. We observed that several genes including *IL-4*, *Mip2*, and *iNos2*

exhibited increased expression in AAV-Hmgb2 mice, but decreased expression in shHmgb2 or ICM mice (Supplemental Figure S4A–C, http://links.lww.com/HC9/A607). However, *Ccl2* and *Tnfα* did not show a consistent regulation by Hmgb2.

HMGB2 is required for stellate cell activation

Since HSCs are considered as a major contributor to liver fibrosis, we investigated the potential role of HSC-resident HMGB2. Primary HSCs were isolated from mouse livers and culture-activated on uncoated plastic dishes and coverslips for 7 days. On day 1, HMGB2 protein was detected in the nucleus of quiescent HSCs (Supplemental Figure S5, http://links.lww.com/HC9/A607). By day 3, we started to observe α-SMA expressing cells (Supplemental Figure S6, http://links.lww.com/HC9/A607), indicating the early activation of HSCs. At day 5 of activation, many cells showed markedly increased staining of α-SMA, and HMGB2 was found mostly in the nucleus (Figure 5A). By day 6 of culture, HSCs became activated by showing further induction of α-SMA (Supplemental Figure S7, http://links.lww.com/HC9/A607). HMGB2 protein was also observed in the cytoplasmic compartment in addition to its nuclear localization by day 7 (Supplemental Figure S8, http://links.lww.com/HC9/A607).

As expected, HSCs isolated from *Hmgb2*$^{-/-}$ mice showed little activation after 5 days of culture compared with WT HSCs (Figure 5B), as indicated by less number of cells with prominent stress fibers and long, flat appearance. It was also associated with a marked reduction of proteins including α-SMA (Figure 5C) and fibronectin (Supplemental Figure S9A, http://links.lww.com/HC9/A607). Interestingly, HMGB1 protein was moderately increased in *Hmgb2*$^{-/-}$ HSCs, suggesting that the inactivation of HSCs is unlikely contributed by HMGB1. In addition, MMP2 and MMP9 protein levels were elevated in *Hmgb2*$^{-/-}$ versus WT HSCs (Supplemental Figure S9A, http://links.lww.com/HC9/A607). Furthermore, serum hydroxyproline levels were increased in WT-CCl_4 versus WT-oil mice, which were decreased in ICM-treated WT mice or *Hmgb2*$^{-/-}$ mice (Figure 5D). Taken together, the results suggest that *Hmgb2* deficiency prevents HSC activation.

To better understand the mechanistic effect of ICM *in vivo*, we analyzed AKT and ERK signaling proteins in mouse livers from WT mice treated with CCl_4 alone or in combination with ICM. Both p-AKT and p-ERK1/2 were downregulated in CCl_4 + ICM versus CCl_4 group

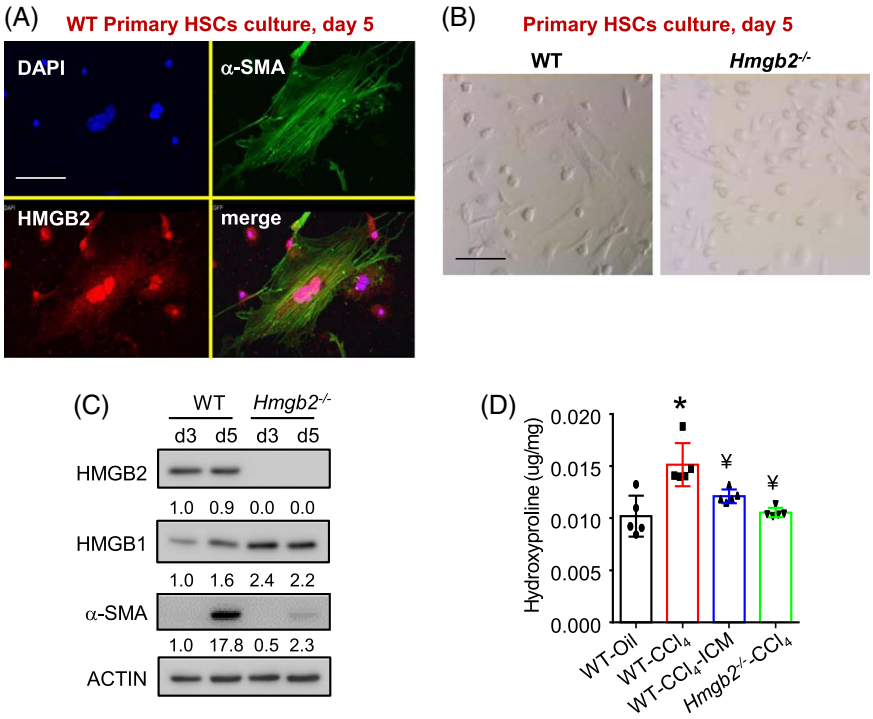

FIGURE 5 *Hmgb2* deficiency impairs the activation of primary mouse HSCs. (A) Representative confocal images of immunofluorescence staining of primary HSCs. HSCs were isolated from WT mice, plated on uncoated plastic dishes, and culture-activated for 5 days. Cells were fixed and immunostained with an anti-α-SMA (green) or an anti-HMGB2 (red) antibody. Scale bar = 50 μm. (B) Representative phase-contrast images of primary HSCs from WT and *Hmgb2*$^{-/-}$. HSCs were culture-activated for 5 days. Scale bar = 50 μm. (C) Western blot of proteins in whole cell lysates from WT and *Hmgb2*$^{-/-}$ primary HSCs culture-activated for 3 or 5 days (n = 5–10 mice/group). (D) Serum hydroxyproline levels. $^{*}p < 0.05$ versus WT-oil; $^{¥}p < 0.05$ versus WT-CCl_4 (n = 5/group). Abbreviations: α-SMA, alpha smooth muscle actin; CCl_4, carbon tetrachloride; HMGB2, high mobility group protein 2; ICM, inflachromene; WT, wild type.

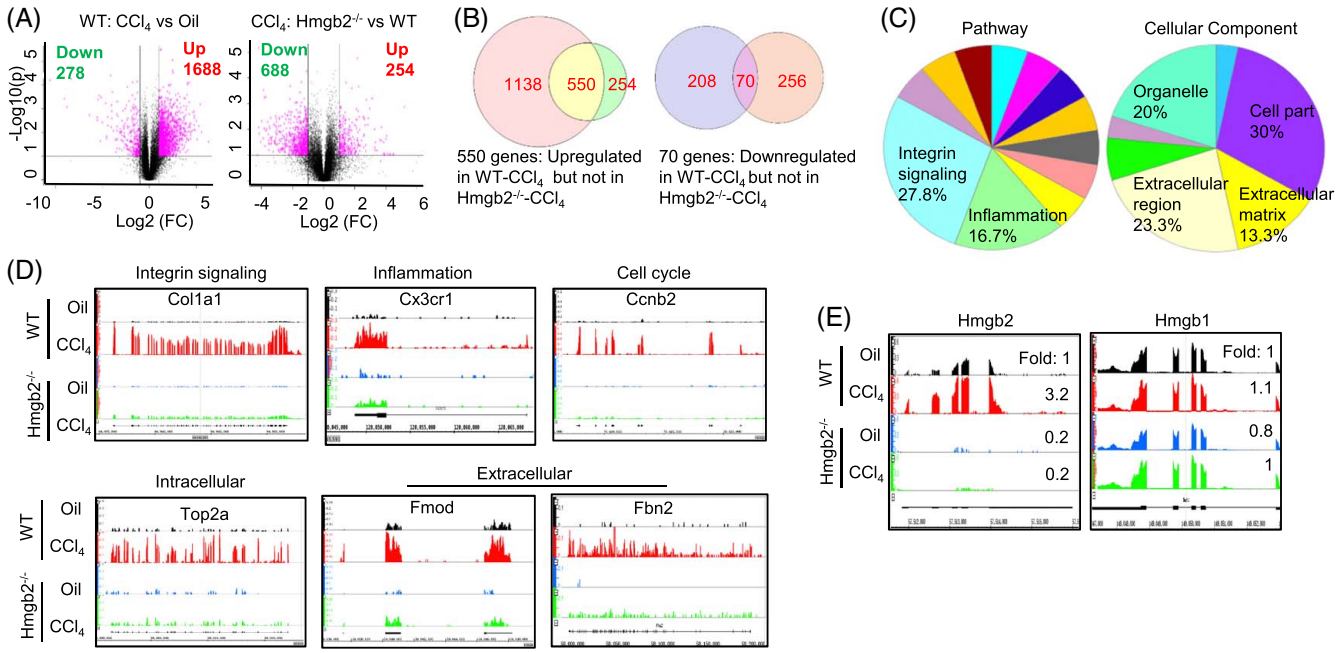

FIGURE 6 RNA-seq identifies new signaling pathways regulated by HMGB2. (A) Volcano plot for differentially expressed genes. The *x*-axis represents a $\log_2$ ratio of gene expression between indicated groups; the *y*-axis represents an adjusted *p*-value based on $-\log_{10}$. The pink dots represent the differentially expressed genes based on $p < 0.1$ and $\log_2$ (FC) > 1. The numbers of upregulated and downregulated genes are indicated. (B) Venn diagram shows the overlap of differentially expressed genes in the indicated groups. Pink: upregulated in WT-CCl_4 versus WT-Oil. Green: downregulated in *Hmgb2*$^{-/-}$-CCl_4 versus WT-CCl_4. Purple: downregulated in WT-CCl_4 versus WT-Oil. Orange: upregulated in *Hmgb2*$^{-/-}$-CCl_4 versus WT-CCl_4. (C) Pathway analysis of significantly changed genes using PANTHER. (D) Visualization of RNA-seq peaks of representative genes from different pathways, including Col1a1, Cx3cr1, Ccnb2, Fmod, DNA Top2a, and Fbn2. (E) Integrated Genome Browser visualization of RNA-seq read tracks for Hmgb2 and Hmgb1 in WT and *Hmgb2*$^{-/-}$ treated with corn oil or CCl_4. The number on the right of each peak view represents the quantification of RPKM relative to WT-Oil, which was set as 1. Abbreviations: CCl_4, carbon tetrachloride; Ccnb2, cyclin B; *Col1a1*, collagen type I alpha; Cx3cr1, C-X3-C motif chemokine receptor 1; Fbn, fibrillin; FC, fold change; Fmod, fibromodulin; HMGB1, high mobility group protein 1; HMGB2, high mobility group protein 2; RPKM, reads per kilobase per million mapped reads; Top2a, topoisomerase 2-alpha; WT, wild type.

(Supplemental Figure S9B, http://links.lww.com/HC9/A607). When HSCs were treated with profibrotic mediators PDGF, RANTES, LPS, and TGF-β1, the activation of p-AKT and p-ERK1/2 proteins by PDGF was evidently diminished in *Hmgb2*$^{-/-}$ versus WT HSCs (Supplemental Figure S9C, http://links.lww.com/HC9/A607). Therefore, HSC inactivation due to *Hmgb2* deficiency was associated with impaired ERK and AKT signaling.

RNA-seq identifies topoisomerase 2-alpha, fibromodulin, and fibrillin as part of the HMGB2-regulated signaling network

To comprehensively explore the regulatory network of HMGB2, we performed RNA-seq on livers from WT-corn oil, WT-CCl_4, *Hmgb2*$^{-/-}$-corn oil, and *Hmgb2*$^{-/-}$-CCl_4 mice. The volcano plot revealed 1966 differentially expressed genes, the majority (86%, 1688 genes) of which appeared upregulated in WT-CCl_4 versus WT-oil (Figure 6A left). In contrast, 688 genes were downregulated in *Hmgb2*$^{-/-}$-CCl_4, compared to WT-CCl_4 (Figure 6A right). The Venn diagram illustrated 550 upregulated genes in WT-CCl_4 mice and the induction of those genes was prevented in *Hmgb2*$^{-/-}$-CCl_4 mice (Figure 6B left). On the contrary, there were 70 genes downregulated in WT-CCl_4 but not in *Hmgb2*$^{-/-}$-CCl_4 (Figure 6B right). GO pathway analysis revealed that 27.8% and 16.7% of the genes were enriched in the pathways of integrin signaling and inflammation (Figure 6C left), respectively. GO cellular component analysis revealed gene enrichment in the clusters of extracellular region (23.3%) and ECM (13.3%) (Figure 6C right). The RNA-seq tracks of representative genes are presented in Figure 6D, including collagen type 1 alpha (*Col1a1*), C-X3-C motif chemokine receptor 1 (*Cx3cr1*), cyclin B2 (*Ccnb2*), DNA topoisomerase 2-alpha (*Top2a*), fibromodulin (*Fmod*), and fibrillin2 (*Fbn2*). As expected, the sequencing reads across exons at the Hmgb2 locus were barely detectable in *Hmgb2*$^{-/-}$-corn oil and *Hmgb2*$^{-/-}$-CCl_4 mice (Figure 6E left), indicating that the RNA-seq data are highly reliable. *Hmgb2* mRNA levels were significantly higher in WT-CCl_4 versus WT-corn oil. In contrast, Hmgb1 mRNA showed moderate changes in response to CCl_4 in WT and *Hmgb2*$^{-/-}$ mice (Figure 6E right).

From the 550 genes, we further identified the top 45 most differentially expressed genes [$\log_2$ (FC) > 1.5, and $p < 0.05$], as presented in the heatmap (Figure 7A). These genes were highly induced by CCl_4 in WT mice,

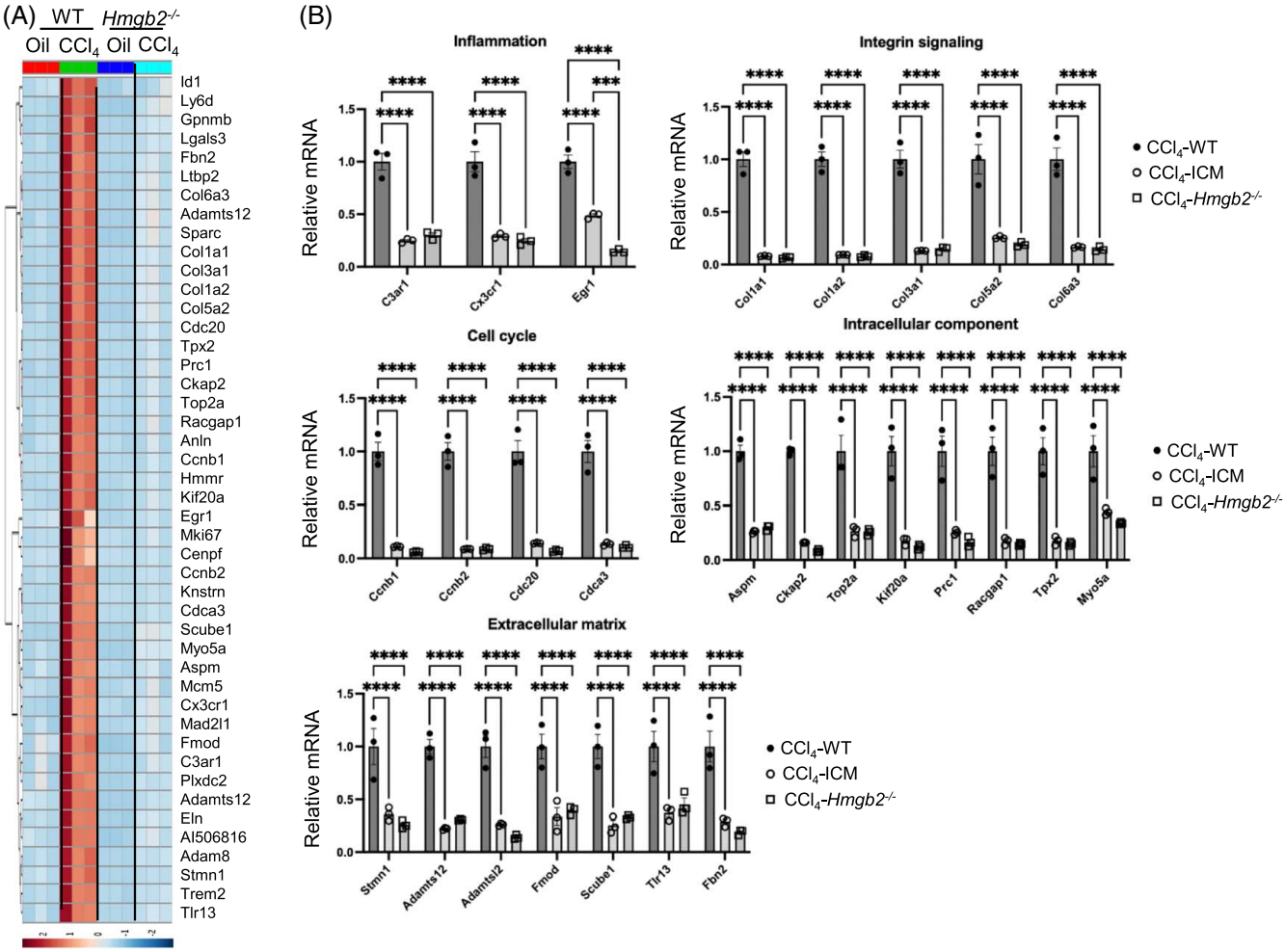

FIGURE 7 Gene networks altered by HMGB2 deficiency. (A) Heatmap of the top 45 differentially expressed genes from the overlapping 550 genes in Figure 6B, with a cutoff of $\log_2$ (FC) > 1.5, $p < 0.05$. The RPKM fold changes in each group were compared to WT-Oil, which was set as 1. (B) Quantitative PCR validation of selected genes in several signaling pathways. Each bar represents triplicate assays from pooled samples from 5 individual mice. Data are shown as mean ± SEM. ***$p < 0.001$; ****$p < 0.0001$ versus indicated group. Abbreviations: CCl_4, carbon tetrachloride; *Col1a1*, collagen type I alpha; Cx3cr1, C-X3-C motif chemokine receptor 1; Fbn, fibrillin; Fmod, fibromodulin; HMGB2, high mobility group protein 2; ICM, inflachromene; RPKM, reads per kilobase per million mapped reads; WT, wild type.

but not in *Hmgb2*$^{-/-}$-corn oil and *Hmgb2*$^{-/-}$-CCl_4 mice. We performed qPCR on selected genes in several signaling pathways (Figure 7B), which validated the RNA-seq results. Protein-protein association analysis revealed an interaction network consisting of *Col3a1*, *Fbn2*, *Fmod*, and collagens (Supplemental Figure S10A, http://links.lww.com/HC9/A607). In addition, a putative interaction network linked HMGB2 to genes in inflammation, cell cycle, and intracellular components, including *Top2α*, *Ccnb*, and *Egr1* (Supplemental Figure

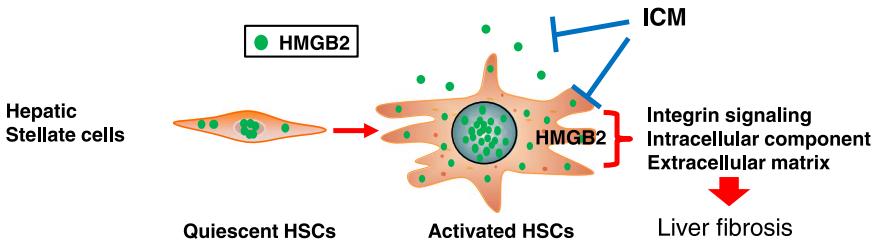

FIGURE 8 Diagram showing HMGB2-mediated regulatory pathways in liver fibrosis. In a normal liver, HMGB2 proteins are expressed in the nucleus of HSCs and to a lesser extent in the cytoplasm. Upon hepatocyte injury by CCl_4, HMGB2 proteins are markedly induced in HSCs, which may facilitate its extracellular secretion. HMGB2 augments the fibrogenic effect of CCl_4 by activating multiple pathways associated with collagen deposition. *Hmgb2*-deficient HSCs showed impaired transdifferentiation and decreased extracellular signal-regulated kinase signaling. ICM reversed liver fibrosis by downregulating HMGB2 protein expression. Abbreviations: HMGB2, high mobility group protein 2; ICM, inflachromene.

S10B, http://links.lww.com/HC9/A607). The results suggest HMGB2 as an important checkpoint to integrate multiple pathways involved in liver fibrosis.

DISCUSSION

In the present study, we provided compelling evidence for a new regulatory role of HMGB2 in liver fibrosis and cirrhosis. HMGB2 expression is highly induced in human NASH, alcohol-associated, and HCV-associated liver cirrhosis, as well as in CCl_4 and ethanol binge–induced liver injury and fibrosis. Genetic ablation of Hmgb2 *in vivo* protects against CCl_4-induced liver fibrosis due to the inactivation of HSCs. Notably, ICM, a small molecule inhibitor of HMGB2, ameliorates CCl_4-induced HMGB2 levels in the liver and plasma and slows down liver fibrosis induced by CCl_4 (Figure 8).

HMGB proteins were initially identified as nuclear nonhistone chromosomal binding proteins that play a role in DNA replication, recombination, transcription, and repair.[7,8] Subsequent studies demonstrated that they can be released to the ECM and function as a damage-associated molecular pattern upon cellular damage.[12–14] An interesting observation is that IL-4, a Th2 type cytokine important for countering type I inflammation,[43] is positively regulated by HMGB2. Although HMGB2 is expressed at very low levels in KCs, knockdown of HMGB2 by shRNA or ICM blunts the response of inflammatory genes *Il-4*, *Mip2*, and *iNos2* to CCl_4. We postulate that the release of HMGB2 from HSCs may elicit a proinflammatory response of KCs through cell-to-cell communications, which will be elucidated in future studies. It should be noted that the sequence homology of HMGB2 and HMGB1 is ~79% and ICM has been reported to bind to both proteins in microglia.[12] Interestingly, ICM inhibits HMGB2 but not HMGB1 protein in mouse liver, suggesting that tissue or cell environment may likely affect its efficacy.

TGF-β1 is a key cytokine mediator in liver fibrogenesis through its receptor to modulate the activity of Smad proteins and activate HSCs, producing fibrotic scar.[44] However, the TGF-β1/Smad pathway was not significantly altered in *Hmgb2*$^{-/-}$ HSCs. Besides TGF-β1, PDGF is considered another critical fibrotic cytokine.[45] Our studies showed that *Hmgb2* deficiency resulted in decreased PDGF signaling with reduced activity of ERK and AKT, 2 known downstream targets of PDGF in activating HSCs. In contrast, the increased HMGB2 expression in response to CCl_4 was accompanied by the increased activity of AKT and ERK, suggesting that PDGF signaling may play a critical role in HMGB2-mediated liver fibrosis. Moreover, upon liver damage, the active HSCs display increased PDGF receptor expression and PDGF release. Based on our findings and others', we propose that HMGB2 is induced in hepatocytes and stellate cells upon liver injury along with PDGF, resulting in the activation of HSCs. Through the signaling networks of AKT and ERK, HSCs undergo transdifferentiation and proliferation, leading to the production and deposition of ECM proteins such as α-SMA, which results in the development of liver fibrosis. Our data do not exclude the possibility that other liver resident cells, for example, the hepatocytes and macrophages, may release signaling molecules in an HMGB2-dependent manner, which may also act on HSCs. Further studies are warranted to identify a detailed mechanism of the cytokine-like function of HMGB2 and cross talk among other liver resident cells in liver fibrogenesis.

Using a transcriptomic high throughput analysis, we identified not only the interaction of HMGB2 with the well-known hepatic fibrogenic signaling pathway, but also genes regulating inflammation, cell cycle, intracellular component, and ECM, including *Fmod*, *Fbn2*, and *Top2α*. *Fbn2* was implicated in extracellular tropoelastin deposition,[46] whereas *Fmod* was reported to regulate liver injury and fibrosis.[47] *Top2α*, on the other hand, was co-upregulated in human HCC with Rac GTPase-activating protein 1 (*Racgap1*);[48] the latter was also identified by our RNA-seq analysis to be co-downregulated with *Top2α* in *Hmgb2*$^{-/-}$ mice. This unbiased approach provides a solid basis to further investigate the HMGB2-regulated signaling network in the development of liver fibrosis in future studies.

In conclusion, we report that HMGB2 is indispensable for stellate cell activation. HMGB2 may serve as a potential therapeutic target to prevent HSC activation during chronic liver injury and the development of liver fibrosis and cirrhosis. The serum HMGB2 induction may also serve as a potential diagnostic marker for liver fibrosis and cirrhosis in human patients.

AUTHOR CONTRIBUTIONS

Li Wang conceived and Dennis Wright, Diane Burgess, Li Wang, and Zhihong Yang supervised the work. Yi Huang, Swetha Rudraiah, Jing Ma, Santosh K. Keshipeddy, Antonio Costa, Yuxia Zhang, and Zhihong Yang performed experiments. Zhihong Yang, Li Wang, Suthat Liangpunsakul, Jing Ma, and Nazmul Huda: prepared or edited the manuscript.

ACKNOWLEDGMENTS

The authors thank Drs Guadalupe Garcia-Tsao and Randolph de la Rosa Rodriguez for sharing human samples through the Yale Silvio O. Conte Digestive Diseases Research Core Center (P30DK034989) and Hidekazu Tsukamoto for providing liver tissues through the Tissue Sharing Program of the Animal Core of the Southern California Research Center for ALPD and Cirrhosis (P50AA011999). The deidentified human liver specimens were obtained from the Liver Tissue Cell Distribution System in Minneapolis, Minnesota (NIH

Contract # HSN276201200017C). Swetha Rudraiah's current affiliation is FDA/CTP. Although the author (Swetha Rudraiah) is a current FDA/CTP employee, this work was not done as part of her official duties. This publication/presentation reflects the views of the author and should not be construed to reflect the FDA/CTP's views or policies.

FUNDING INFORMATION

Zhihong Yang is supported by the Central Society for Clinical and Translational Research (CSCTR).

CONFLICTS OF INTEREST

The authors have no conflicts to report.

ORCID

Nazmul Huda https://orcid.org/0000–0002–7788–8621
Zhihong Yang https://orcid.org/0000–0001–6199–3956

REFERENCES

1. Friedman SL. Evolving challenges in hepatic fibrosis. Nat Rev Gastroenterol Hepatol. 2010;7:425–36.
2. Kawada N. Evolution of hepatic fibrosis research. Hepatol Res. 2011;41:199–208.
3. Gressner AM, Weiskirchen R. Modern pathogenetic concepts of liver fibrosis suggest stellate cells and TGF-beta as major players and therapeutic targets. J Cell Mol Med. 2006;10:76–99.
4. Furukawa F, Matsuzaki K, Mori S, Tahashi Y, Yoshida K, Sugano Y, et al. p38 MAPK mediates fibrogenic signal through Smad3 phosphorylation in rat myofibroblasts. Hepatology. 2003;38:879–9.
5. Pannu J, Nakerakanti S, Smith E, ten Dijke P, Trojanowska M. Transforming growth factor-beta receptor type I-dependent fibrogenic gene program is mediated via activation of Smad1 and ERK1/2 pathways. J Biol Chem. 2007;282:10405–3.
6. De Minicis S, Svegliati-Baroni G. Fibrogenesis in nonalcoholic steatohepatitis. Expert Rev Gastroenterol Hepatol. 2011;5:179–87.
7. Malarkey CS, Churchill ME. The high mobility group box: the ultimate utility player of a cell. Trends Biochem Sci. 2012;37:553–62.
8. Thomas JO, Travers AA. HMG1 and 2, and related 'architectural' DNA-binding proteins. Trends Biochem Sci. 2001;26:167–74.
9. Zhao Y, Yang Z, Wu J, Wu R, Keshipeddy SK, Wright D, et al. High-mobility-group protein 2 regulated by microRNA-127 and small heterodimer partner modulates pluripotency of mouse embryonic stem cells and liver tumor initiating cells. Hepatol Commun. 2017;1:816–30.
10. Fan Z, Beresford PJ, Zhang D, Lieberman J. HMG2 interacts with the nucleosome assembly protein SET and is a target of the cytotoxic T-lymphocyte protease granzyme A. Mol Cell Biol. 2002;22:2810–0.
11. Boonyaratanakornkit V, Melvin V, Prendergast P, Altmann M, Ronfani L, Bianchi ME, et al. High-mobility group chromatin proteins 1 and 2 functionally interact with steroid hormone receptors to enhance their DNA binding in vitro and transcriptional activity in mammalian cells. Mol Cell Biol. 1998;18:4471–87.
12. Lee S, Nam Y, Koo JY, Lim D, Park J, Ock J, et al. A small molecule binding HMGB1 and HMGB2 inhibits microglia-mediated neuroinflammation. Nat Chem Biol. 2014;10:1055–60.
13. Ueno H, Matsuda T, Hashimoto S, Amaya F, Kitamura Y, Tanaka M, et al. Contributions of high mobility group box protein in experimental and clinical acute lung injury. Am J Respir Crit Care Med. 2004;170:1310–6.
14. Pusterla T, de Marchis F, Palumbo R, Bianchi ME. High mobility group B2 is secreted by myeloid cells and has mitogenic and chemoattractant activities similar to high mobility group B1. Autoimmunity. 2009;42:308–10.
15. Ronfani L, Ferraguti M, Croci L, Ovitt CE, Scholer HR, Consalez GG, et al. Reduced fertility and spermatogenesis defects in mice lacking chromosomal protein Hmgb2. Development. 2001;128:1265–73.
16. Taniguchi N, Carames B, Ronfani L, Ulmer U, Komiya S, Bianchi ME, et al. Aging-related loss of the chromatin protein HMGB2 in articular cartilage is linked to reduced cellularity and osteoarthritis. Proc Natl Acad Sci U S A. 2009;106:1181–6.
17. Zhou X, Li M, Huang H, Chen K, Yuan Z, Zhang Y, et al. HMGB2 regulates satellite cell-mediated skeletal muscle regeneration via IGF2BP2. J Cell Sci. 2016;129:4305–16.
18. Kwon JH, Kim J, Park JY, Hong SM, Park CW, Hong SJ, et al. Overexpression of high-mobility group box 2 is associated with tumor aggressiveness and prognosis of hepatocellular carcinoma. Clin Cancer Res. 2010;16:5511–21.
19. Zhang Y, Xu N, Xu J, Kong B, Copple B, Guo GL, et al. E2F1 is a novel fibrogenic gene that regulates cholestatic liver fibrosis through the Egr-1/SHP/EID1 network. Hepatology. 2014;60:919–30.
20. Smalling RL, Delker DA, Zhang Y, Nieto N, McGuiness MS, Liu S, et al. Genome-wide transcriptome analysis identifies novel gene signatures implicated in human chronic liver disease. Am J Physiol Gastrointest Liver Physiol. 2013;305:G364–74.
21. Zhang Y, Liu C, Barbier O, Smalling R, Tsuchiya H, Lee S, et al. Bcl2 is a critical regulator of bile acid homeostasis by dictating Shp and lncRNA H19 function. Sci Rep. 2016;6:20559.
22. Yang Z, Kusumanchi P, Ross RA, Heathers L, Chandler K, Oshodi A, et al. Serum metabolomic profiling identifies key metabolic signatures associated with pathogenesis of alcoholic liver disease in humans. Hepatol Commun. 2019;3:542–7.
23. Yang Z, Ross RA, Zhao S, Tu W, Liangpunsakul S, Wang L. LncRNA AK054921 and AK128652 are potential serum biomarkers and predictors of patient survival with alcoholic cirrhosis. Hepatol Commun. 2017;1:513–23.
24. Kwon HJ, Won YS, Park O, Chang B, Duryee MJ, Thiele GE, et al. Aldehyde dehydrogenase 2 deficiency ameliorates alcoholic fatty liver but worsens liver inflammation and fibrosis in mice. Hepatology. 2014;60:146–57.
25. Lazaro R, Wu R, Lee S, Zhu NL, Chen CL, French SW, et al. Osteopontin deficiency does not prevent but promotes alcoholic neutrophilic hepatitis in mice. Hepatology. 2015;61:129–40.
26. Liu C, Yang Z, Wu J, Zhang L, Lee S, Shin DJ, et al. Long noncoding RNA H19 interacts with polypyrimidine tract-binding protein 1 to reprogram hepatic lipid homeostasis. Hepatology. 2018;67:1768–83.
27. Costa AP, Xu X, Khan MA, Burgess DJ. Liposome formation using a coaxial turbulent jet in co-flow. Pharm Res. 2016;33:404–16.
28. Yang Z, Tsuchiya H, Zhang Y, Lee S, Liu C, Huang Y, et al. REV-ERBalpha activates C/EBP homologous protein to control small heterodimer partner-mediated oscillation of alcoholic fatty liver. Am J Pathol. 2016;186:2909–0.
29. Zhang L, Yang Z, Trottier J, Barbier O, Wang L. Long noncoding RNA MEG3 induces cholestatic liver injury by interaction with PTBP1 to facilitate shp mRNA decay. Hepatology. 2017;65:604–15.
30. Lopez-Sanchez I, Dunkel Y, Roh YS, Mittal Y, De Minicis S, Muranyi A, et al. GIV/girdin is a central hub for profibrogenic signalling networks during liver fibrosis. Nat Commun. 2014;5:4451.
31. Xu L, Hui AY, Albanis E, Arthur MJ, O'Byrne SM, Blaner WS, et al. Human hepatic stellate cell lines, LX-1 and LX-2: New tools for analysis of hepatic fibrosis. Gut. 2005;54:142–51.

32. Lee SM, Zhang Y, Tsuchiya H, Smalling R, Jetten AM, Wang L. Small heterodimer partner/neuronal PAS domain protein 2 axis regulates the oscillation of liver lipid metabolism. Hepatology. 2015;61:497–505.
33. Tsuchiya H, da Costa KA, Lee S, Renga B, Jaeschke H, Yang Z, et al. Interactions between nuclear receptor SHP and FOXA1 maintain oscillatory homocysteine homeostasis in mice. Gastroenterology. 2015;148:1012–23 e1014.
34. Zhou T, Zhang Y, Macchiarulo A, Yang Z, Cellanetti M, Coto E, et al. Novel polymorphisms of nuclear receptor SHP associated with functional and structural changes. J Biol Chem. 2010;285:24871–81.
35. Zhang Y, Andrews GK, Wang L. Zinc-induced Dnmt1 expression involves antagonism between MTF-1 and nuclear receptor SHP. Nucleic Acids Res. 2012;40:4850–60.
36. Zhang Y, Wang L. Nuclear receptor SHP inhibition of Dnmt1 expression via ERRgamma. FEBS Lett. 2011;585:1269–75.
37. Choiniere J, Wu J, Wang L. Pyruvate dehydrogenase kinase 4 deficiency results in expedited cellular proliferation through E2F1-mediated increase of cyclins. Mol Pharmacol. 2017;91:189–96.
38. Yang Z, Koehler AN, Wang L. A novel small molecule activator of nuclear receptor SHP inhibits HCC cell migration via suppressing Ccl2. Mol Cancer Ther. 2016;15:2294–301.
39. Song Y, Liu C, Liu X, Trottier J, Beaudoin M, Zhang L, et al. H19 promotes cholestatic liver fibrosis by preventing ZEB1-mediated inhibition of epithelial cell adhesion molecule. Hepatology. 2017; 66:1183–96.
40. Tran M, Lee SM, Shin DJ, Wang L. Loss of miR-141/200c ameliorates hepatic steatosis and inflammation by reprogramming multiple signaling pathways in NASH. JCI Insight. 2017;2: e96094.
41. Zincarelli C, Soltys S, Rengo G, Rabinowitz JE. Analysis of AAV serotypes 1-9 mediated gene expression and tropism in mice after systemic injection. Mol Ther. 2008;16:1073–80.
42. Sato Y, Murase K, Kato J, Kobune M, Sato T, Kawano Y, et al. Resolution of liver cirrhosis using vitamin A-coupled liposomes to deliver siRNA against a collagen-specific chaperone. Nat Biotechnol. 2008;26:431–2.
43. Lopez-Navarrete G, Ramos-Martinez E, Suarez-Alvarez K, Aguirre-Garcia J, Ledezma-Soto Y, Leon-Cabrera S, et al. Th2-associated alternative Kupffer cell activation promotes liver fibrosis without inducing local inflammation. Int J Biol Sci. 2011;7: 1273–86.
44. Dooley S, ten Dijke P. TGF-beta in progression of liver disease. Cell Tissue Res. 2012;347:245–56.
45. Borkham-Kamphorst E, Kovalenko E, van Roeyen CR, Gassler N, Bomble M, Ostendorf T, et al. Platelet-derived growth factor isoform expression in carbon tetrachloride-induced chronic liver injury. Lab Invest. 2008;88:1090–100.
46. Kanta J. Elastin in the liver. Front Physiol. 2016;7:491.
47. Mormone E, Lu Y, Ge X, Fiel MI, Nieto N. Fibromodulin, an oxidative stress-sensitive proteoglycan, regulates the fibrogenic response to liver injury in mice. Gastroenterology. 2012;142: 612–21 e615.
48. Drozdov I, Bornschein J, Wex T, Valeyev NV, Tsoka S, Malfertheiner P. Functional and topological properties in hepatocellular carcinoma transcriptome. PLoS One. 2012;7:e35510.

How to cite this article: Huang Y, Liangpunsakul S, Rudraiah S, Ma J, Keshipeddy SK, Wright D, et al. HMGB2 is a potential diagnostic marker and therapeutic target for liver fibrosis and cirrhosis. Hepatol Commun. 2023;7:e0299. https://doi.org/10.1097/HC9.0000000000000299